Synthesis and photoluminescence properties of ion-doped $Bi_4Si_3O_{12}$ microcrystals

XUEFENG XIAO [a,b,c,*], HAICHENG WEI[a,b], JIAYUE XU[d], HUAN ZHANG[a,b], XUEFENG ZHANG[e]
[a]*Key Laboratory of Physics and Photoelectric Information Functional Materials Sciences and Technology, North Minzu University, Yinchuan, 750021, China*
[b]*College of Electric and Information Engineering, North Minzu University, Yinchuan, 750021, China*
[c]*School of Materials Science and Engineering, Tongji University, Shanghai 201804, China*
[d]*School of Materials Science and Engineering, Shanghai Institute of Technology, Shanghai, 201804, China*
[e]*Ningxia Ju Jing Yuan Crystal Technology Company Limited, Shizuishan 753000, China*

In this work, the bismuth silicate ($Bi_4Si_3O_{12}$, BSO) microcrystalline were synthesized via a solid state reaction. The structure and the lattice constant of BSO microcrystalline were studied by the X-ray diffraction patterns (XRD). The emission and excitation spectra of BSO microcrystalline doped with 0.05 mol% of trivalent rare-earth and transition metal element ions were also investigated. The research results revealed that the radius of rare-earth ions could influence the light output of BSO microcrystalline and the luminescence intensity of Eu^{3+}-doped microcrystalline was significantly enhanced. The results showed that the radius of doped rare earth ions was an important factor for affecting the luminescence intensity of BSO microcrystalline. It has an important guiding significance for the research of luminescence properties of BSO crystal doped with rare earth and the performance of dual-readout, as well as has important reference value for rare earth doped other crystals research.

(Received March 7, 2018; accepted November 29, 2018)

Keywords: $Bi_4Si_3O_{12}$, Rare earth, Spectral properties, Transition metal ions, Photoluminescence

1. Introduction

Bismuth silicate ($Bi_4Si_3O_{12}$, BSO) is known as an excellent scintillator for various applications in high energy physics, nuclear physics, medical imaging, geological prospecting and other industries due to its advantages of much faster decay time, higher radiation hardness and lower cost [1-4]. BSO crystal has been successfully grown by the modified Bridgman method and its optical properties were also reported [3–5]. Recent studies [2] show that the BSO crystals are excellent materials to be used in 4 π electromagnetic calorimeters in the energy region of several hundreds of millions electron volts. What is more, BSO crystal has potential application in dual-readout calorimeter and has better performances than $Bi_4Ge_3O_{12}$ (BGO) used for dual readout [6–8]. It's easy to separate the Cherenkov and scintillation light for BSO crystal since the short-wavelength cut-off of BSO crystal is small in comparison with BGO crystal.

The properties of BSO crystal can be further optimized by doping rare earth ions [6,9-12]. Research results [13] show that the radius of doping rare earth ions will influence the luminescence characteristics of rare earth-doped BSO crystals. In order to better research the characteristics of fluorescence spectra and absorption edge in of rare earth ions-doped BSO crystals. In this paper, the ion-doped BSO polycrystalline powders were synthesized by solid state reaction and their photoluminescence properties were also studied. The fluorescence spectrum were measured and the ions in the BSO powders excitation and emission spectra of ion transition ways are analyzed, the influence of ion radius is discussed for luminescence mechanism.

2. Experimental

2.1. Synthesis BSO microcrystals

Rare-earth (Gd^{3+},Yb^{3+}, Ho^{3+}, Y^{3+}, Tm^{3+} and Eu^{3+}) and transition metal (Fe^{3+} and Ti^{4+}) ions-doped BSO microcrystals were synthesized by the solid state reaction. The compounds powers with purity of 99.99% were used as starting materials. After drying at 200 ^oC for 3 h, they were accurately weighed according to the formula of $(Bi_{0.995}\text{Rare-earth ions}_{0.005})_4Si_3O_{12}$ and $Bi_4(Si_{0.995}\text{Transition metal ions}_{0.005})_3O_{12}$. All the compounds were mixed and ground in a ball mill coated with polyethylene for 8 h. The mixtures were firstly pressed into cylinders and sintered at 900 ℃ for 5 h to form the BSO polycrystalline. Then, the polycrystalline materials were mixed and ground in a ball mill for another 8 h and the mixtures were pressed into cylinders again and sintered at 950 ℃ for 10 h until the compounds completely form the BSO polycrystalline powders materials. After ground into powders, the mixtures were pressed and sintered again at 950 ℃ for 10 h. After the twice sintering process, the compounds form the BSO polycrystalline powders materials completely.

2.2. Characterizations and methods

The as-synthesized microcrystals were prepared for characterizations. Powder X-ray diffraction (XRD) was performed to examine the phase structure of the as-synthesized polycrystals using a D/max-2200 type diffractometer (Rigaku Co. Ltd., Tokyo, Japan) at room temperature. Absorption spectra were recorded in the range from 100 nm to 800 nm using a Perking–Elmer UV–VIS–NIR spectrophotometer at room temperature. The excitation and fluorescence spectra at room temperature were carried out with Edinburgh Instruments FLS920 spectrophotometer using Xenon lamp as a light source.

3. Results and discussions

3.1. Structure of BSO microcrystals

The XRD patterns of the rare-earth (Gd^{3+}, Yb^{3+}, $Ho^{3+,}$ Y^{3+}, Tm^{3+} and Eu^{3+}) and transition metal (Fe^{3+} and Ti^{4+}) ions-doped BSO microcrystalline are shown in Fig. 1 and Fig. 2. The XRD patterns of the samples indicate that they could be indexed to the orthorhombic structured BSO (PDF#33-0215). No impurity phase such as Gd_2O_3, Yb_2O_3, Ho_2O_3, Y_2O_3, Tm_2O_3, Eu_2O_3, Fe_2O_3 and TiO_2 was detected in the sample. The small shift of position for the diffraction peaks is attributed to the lattice distortion resulted from the accommodation of rare-earth and transition metal ions in the BSO lattices. The lattice constants of the as-synthesized rare-earth and transition metal ions-doped BSO microcrystalline calculated based on the XRD results are summarized in Table 1.

Table 1. The Lattice constants of the as-synthetic rare-earth and transition metal ions doped BSO microcrystalline calculated from the XRD patterns

Lattice Constants	PDF#33-0215-$Bi_4Si_3O_{12}$	BSO	BSO:Ti	BSO:Tm	BSO:Yb	BSO:Y	BSO:Eu	BSO:Fe	BSO:Gd	BSO:Ho
a=b=c (nm)	1.0291	1.02803	1.02867	1.028842	1.028903	1.029035	1.029318	1.028807	1.028973	1.029042
esd	0	0.000831	0.000685	0.000782	0.000906	0.000815	0.00067	0.000393	0.000679	0.000534
Vol(nm^3)	1.08987	1.08647	1.0885	1.08905	1.08924	1.08966	1.09056	1.08893	1.08946	1.08968

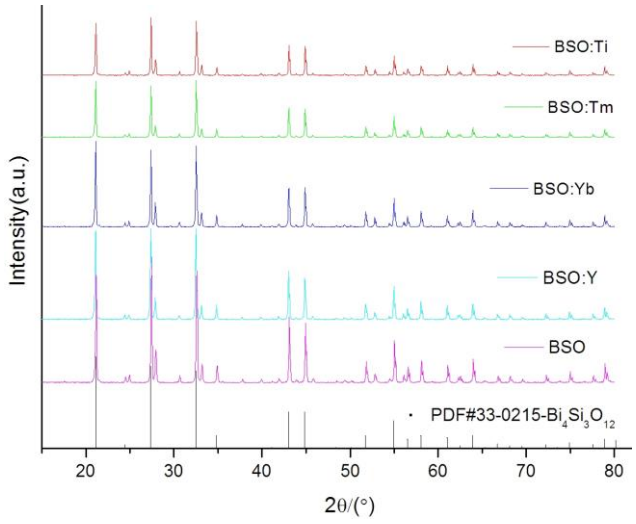

Fig. 1. XRD patterns of the BSO (Ti^{4+}, Tm^{3+},Yb^{3+} and Y^{3+} ions doped BSO) microcrystalline materials

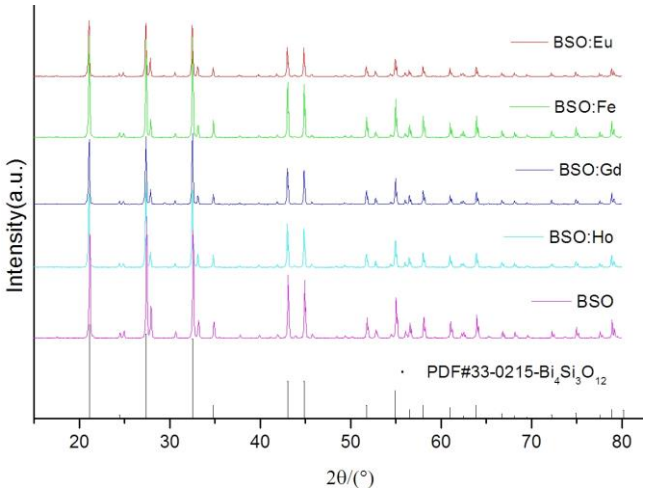

Fig. 2. XRD patterns of the BSO (Eu^{3+}, Fe^{3+}, Gd^{3+} and Ho^{3+} ions doped BSO) microcrystalline materials

3.2. Excitation spectra of ions-doped BSO microcrystalline

Fig. 3 shows the excitation spectrum of the transition metal ions (Fe^{3+}, λ_{em}=483 nm and Ti^{4+}, λ_{em}=488 nm) -doped BSO microcrystalline. The excitation spectrum is mainly in the range of 230 nm-290 nm. The results also show that the excitation intensity is a bit lower than that of pure BSO microcrystalline (λ_{em}=480 nm). Fig. 4 shows the excitation spectra of rare earth ions-doped BSO microcrystalline. The excitation intensity is slightly lower than that of pure BSO microcrystalline (λ_{em}=480 nm). However, the excitation intensity of part of the rare earth ions-doped BSO microcrystalline (like Eu^{3+} ions) increases significantly compared with that of the transition metal ions-doped. In addition, there are still a series of weak excitation peaks in the spectra of pure BSO microcrystalline and Eu^{3+} -doped BSO microcrystalline, and the peak position is slightly different each other. Thus the excitation intensity and peak position could be adjusted because of the doped ions.

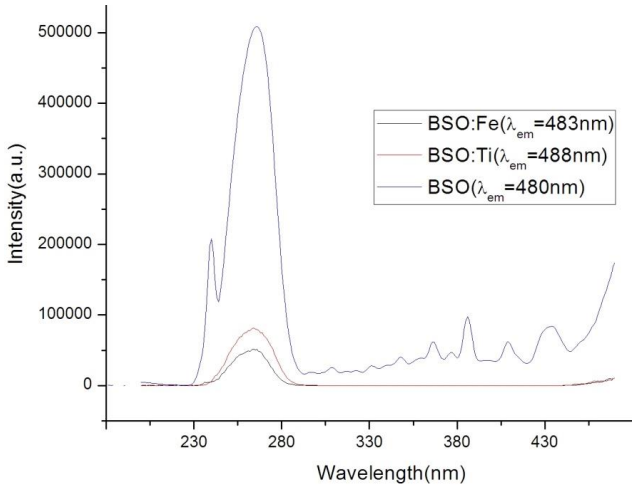

Fig. 3. The excitation spectrum of the transition metal ions (Fe^{3+} and Ti^{4+}) doped BSO icrocrystalline

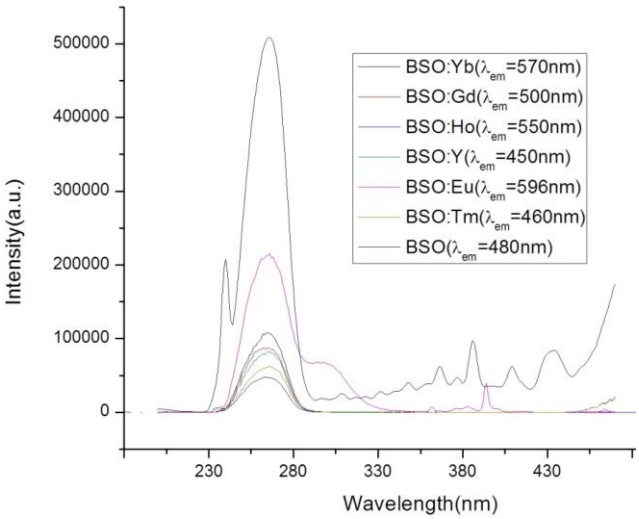

Fig. 4. The excitation spectra of rare earth ions doped BSO microcrystalline

3.3. Emission spectra of ions-doped BSO microcrystalline

The ions or atoms can replace each other in the lattice without destroying the structure of original crystal and form the isomorphic replacement if their nature valence and radius close to each other. Thus, Ti^{4+} and Fe^{3+} ions are able to replace Si^{4+} and the rare earth ions could replace the Bi^{3+} ion in doped BSO microcrystalline. The crystal luminescence performance is thus affected based on the substitution mechanism. Fig. 5 shows the emission spectrum of transition metal ions (Fe^{3+} and Ti^{4+}) -doped BSO microcrystalline. The results indicate the luminescence intensity is significantly lower than that of pure BSO microcrystalline. According to the valence and ionic radius data in Table 2, Ti^{4+} ion could more easily replace Si^{4+} ion, and the crystal structure is thus changed and the luminescence efficiency of Bi^{3+} ions is affected. Similarly, Fe^{3+} ion could more easily replace Si^{4+} ion, and trivalent Fe ions is able to replace a small amount of Bi^{3+} ions, too. Thus the intrinsic luminescence of Bi^{3+} ions is reduced, and Fe^{3+} ion itself does not shine. So the luminescence intensity is decreased obviously compared with that of the Ti^{4+} ion-doped. From Fig. 6, we can see that the luminescence intensity of the Eu^{3+}-doped BSO microcrystalline are increased obviously compared with that of the pure BSO microcrystalline. It can be observed from Fig. 7 that the luminescene intensity of Gd^{3+} ions-doped BSO crystallite is slightly lower than that of the pure BSO microcrystalline, and a shift towards long wave peak. According to the valence and ionic radius data in Table 2, the rare earth ions more easily replace the Bi^{3+} ions in the doped BSO microcrystalline. Comparison of rare earth ions and Bi ionic radius, the ionic radius of Eu^{3+} ion is closest to Bi^{3+}, and Gd^{3+} ion is second. Thus, it can be concluded that the radius of rare earth ions can affect the luminescence intensity of BSO crystal [10].

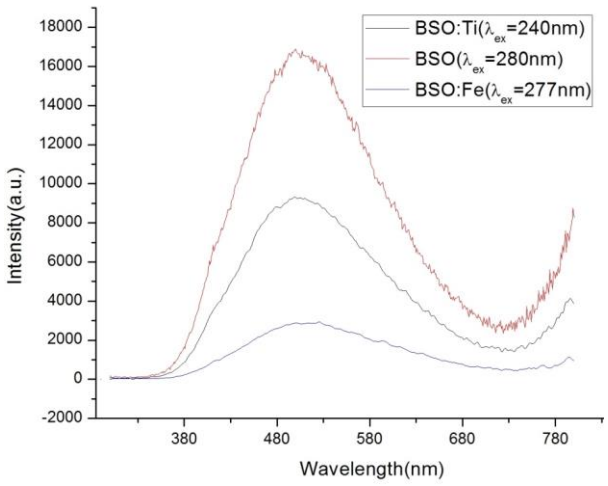

Fig. 5. The emission spectrum of transition metal ions (Fe^{3+} and Ti^{4+}) doped BSO microcrystalline

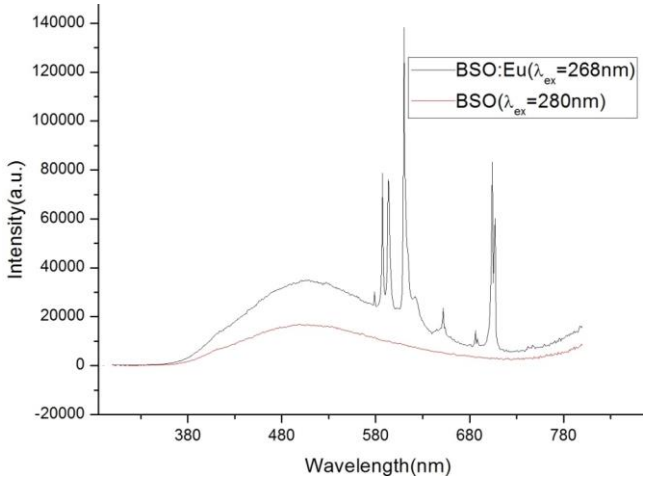

Fig. 6. The emission spectrum of the rare earth Eu^{3+} ions doped BSO microcrystalline

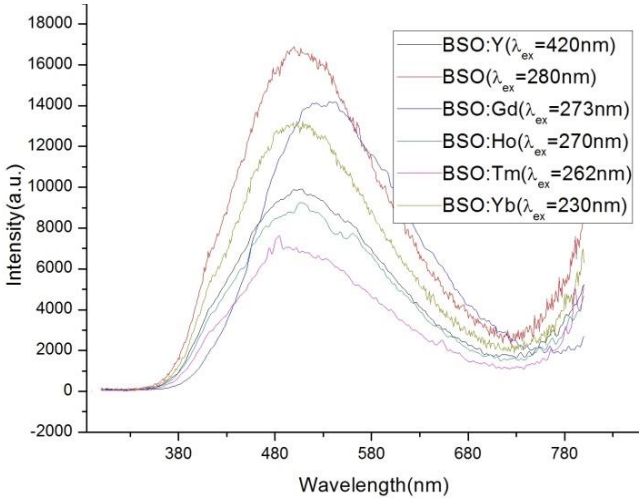

Fig. 7. The emission spectrum of rare earth ions (Gd^{3+}, Yb^{3+}, Ho^{3+}, Y^{3+}, and Tm3+) doped BSO microcrystalline

Table 2. Radius and valence of ions (from the periodic table)

Ions	Ionic radius (nm)	Valence
Si^{4+}	0.040	+4
Bi^{3+}	0.0103	+3
Yb^{3+}	0.0858	+3
Eu^{3+}	0.0947	+3
Ho^{3+}	0.0901	+3
Gd^{3+}	0.0938	+3
Tm^{3+}	0.0869	+3
Y^{3+}	0.09	+3
Ti^{4+}	0.0605	+4
Fe^{3+}	0.0645	+3

3.4. Excitation and emission spectra of Eu^{3+}-doped BSO microcrystalline

Fig. 8 shows the emission and excitation spectra of Eu^{3+}-doped BSO microcrystalline. The excitation and emission peak is at 268 nm and 614 nm, respectively. There are a series of spectral lines in the emission spectrum corresponding to the transition energy levels of Eu^{3+} [14, 15] as shown in Table 3.

Table 3. Suggested transitions between Eu^{3+} energy levels

Wavelength(nm)	Assignment($^S L_J$)
590	$^5D_0 \rightarrow {}^7F_1$
610	$^5D_0 \rightarrow {}^7F_2$
650	$^5D_0 \rightarrow {}^7F_4$
705	$^5D_0 \rightarrow {}^7F_5$

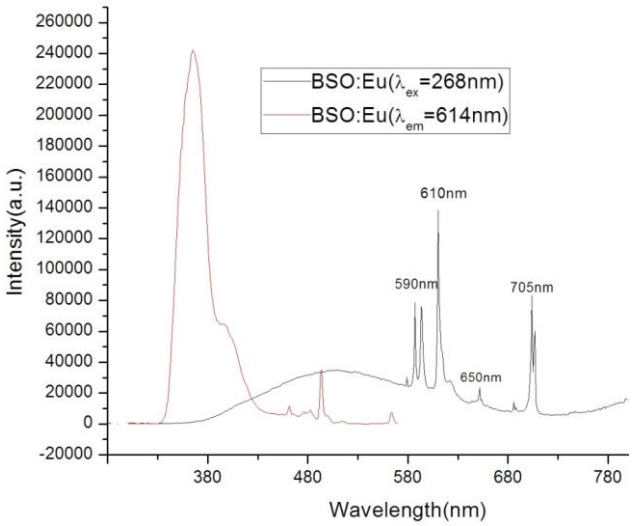

Fig. 8. The emission and excitation spectra of Eu^{3+} doped BSO microcrystalline

4. Conclusions

BSO microcrystalline doped with rare-earth (Gd^{3+}, Yb^{3+}, Ho^{3+}, Y^{3+}, Tm^{3+} and Eu^{3+}) and transition metal (Fe^{3+} and Ti^{4+}) ions were synthesized by many times sintering method. The structure and lattice constant of doped BSO microcrystalline were studied by the XRD patterns. The excitation and emission spectra of doped BSO microcrystalline were measured, and the Eu^{3+} ion transition energy level was given. The luminescence intensity of transition metal ions-doped BSO microcrystalline was significantly lower than that of pure BSO microcrystalline based on the replace mechanism. The luminescence intensity of Eu^{3+}-doped BSO microcrystalline was significantly promoted. The results showed that the radius of doped rare earth ions was an important factor for affecting the luminescence intensity of

BSO microcrystalline. It has an important guiding significance for the research of luminescence properties of BSO crystal doped with rare earth and the performance of dual-readout, as well as has important reference value for rare earth doped other crystals research.

Acknowledgments

This work is supported by Ningxia college scientific research project (No. NGY2017161), Ningxia first-class discipline and scientific research projects (electronic science and technology, No.NXYLXK2017A07), the National Key Basic Research Program (No.2011CB612310), National Natural Science Foundation of China (No. 51342007, 51572175, 61461001), Natural Science Foundation of Ningxia (No. NZ17104), Key Laboratory of North Minzu University (intelligent perception control) and the Ningxia Province Key Research and Development Program (2018BEE03015).

References

[1] J. T. He, G. Y. Zhu, D. B. Chen, X. L. Dong, Z. B. Li, J. G. Bian, S. J. Fan, R. Y. Sun, Y. F. Lin, Y. T. Fei, J. Y. Xu, High Energ. Phys. Nuc. **21**, 886 (1996).

[2] H. Shimizu, F. Miyahara, H. Hariu, T. Hayakawa, T. Ishikawa, M. Itaya, Iwata, T. Kinoshita, T. M. Moriya, T. Nakabayashi, T. Sasaki, Y. Tajima, S. Takita, M. Yamamoto, H. Yamazaki, H. Y. Yoshida, Y. Yoshida, Nucl. Instrum. Methods Phys. Res. Sect. A **550**, 258 (2005).

[3] H. Shen, J. Y. Xu, W. J. Ping, Q. B. He, Y. Zhang, M. Jin, G. J. Jiang, Chinese Phy. Lett. **29**, 076501 (2012).

[4] Y. Zhang, J. Y. Xu, P. F. Shao, J. Cryst. Growth **318**, 920 (2011).

[5] H. Jiang, J. K. Hong, R. Gul, C. Jong Kyu, Nucl. Instrum. Methods Phys. Res. Sect. A **648**, 73 (2011).

[6] X. F. Xiao, J. Y. Xu, W. D. Xiang, J. Inorg. Mater. **28**, 347 (2013).

[7] T. Ishikawa, H. Fujimura, R. Hashimoto, S. Kaida, J. Kasagi, R. Kitazawa, S. Kuwasaki, A. Nakamura, K. Nawa, Y. Okada, M. Sato, H. Shimizu, K. Suzuki, Y. Tajima, S. Takahashi, Y. Tsuchikawa, H. Yamazaki, H. Y. Yoshida, Nucl. Instrum. Methods Phys. Res. Sect. A **694**, 348 (2012).

[8] N. Akchurin, F. Bedeschi, A. Cardini, M. Cascella, G. Ciapetti, D. De Pedis, M. Fasoli, R. Ferrari, S. Franchino, M. Fraternali, G. Gaudio, J. Hauptman, M. Incagli, F. Lacava, L. La Rotonda, S. Lee, M. Livani, E. Meoni, A. Negri, D. Pinci, A. Policicchio, F. Scuri, A. Sill, G. Susinno, T. Venturelli, C. Voena, R. Wigmans, Nucl. Instrum. Methods Phys. Res. Sect. A **640**, 91 (2011).

[9] B. B. Yang, J. Y. Xu, Y. Zhang, H. B. Zeng, T. Tian, Y. Q. Chu, Y. B. Pan, Q. Z. Cui. Instrum. Methods Phys. Res. Sect. A **807**, 1 (2016).

[10] T. Tian, H. W. Feng, Y. Zhang, D. Zhou, H. Shen, H. C. Wang, J. Y. Xu, Crystals **7**, 8 (2017).

[11] J. Y. Xu, J. Wang, W. Chen, X. F. Xiao, B. B. Yang, Z. Y. Wang, F. Li, H. D. Xie, J. Inorg. Mater. **31**, 1147 (2016).

[12] X. F. Xiao, J. Y. Xu, H. C. Wei, Y. Q. Chu, B. B. Yang, X. F. Zhang, J Rare Earth, in press. https://doi.org/10.1016/j.jre.2018.05.022.

[13] P. D. Townsend, A. K. Jazmati, T. Karali, M. Maghrabi, S. G. Raymond, B. Yang, J. Phys. Condens. Mat. **13**, 2211 (2001).

[14] S. G. Raymond, P. D. Townsend, J. Phys. Condens. Mat. **12**, 2103 (2000).

[15] Y. T. Arslanlar, Z. Kotan, R. Kibar, N. Can, Spectrosc. Lett. **46**, 590 (2013).

*Corresponding author: xxf666666@163.com